



STUDY ON USAGE OF PRV METRICS FOR HEART HEALTH ASSESSMENT: A TIME-BASED SYSTEMATIC INVESTIGATION

¹Simhadri.V,²Veera Meghana.Ch,³Satya Jyothi.T, ⁴Pavan Kumar. K,⁵Ajay Ganeshmanikanta. S

¹Assistant Professor Dept of ECE, Godavari Institute of Engineering and Technology(A),Rajahmundry,AP

^{2,3,4,5}Students Dept of ECE, Godavari Institute of Engineering and Technology (A), Rajahmundry, AP

Abstract-The research work presented here discusses the pulse rate variability analysis using the photoplethysmogram signals (PPG) signals. Pulsatile signals, can be used to extract pulse rate variability (PRV), which describes changes in pulse rate over time. PRV analysis is made quicker and simpler to this research's contribution to PRV analysis. An automatic PRV detection algorithm developed is analyses the PPG signals to identify ectopic beats and correct any errors made during the detection procedure. In presented works mainly works on various time segmented PPG signals recorded under various ambulatory conditions. Presented works also will be evaluated by compiling a database of normal person pulses and a database of heart patient pulses and comparing them according to various signal variation lengths with the metrics values for better cardiac system assesment. Here we have taken reference signals from different data bases using PHYSIO BANK ATM. This is done in consideration of the pulse rate variability (PRV) metrics such as measures in the time domain (AVNN, SDNN, SDDSD, RMSSD, pNN20, pNN50, PPAVG) and the frequency domain (VLF, LF, HF, LF/HF ratio, total power). When everything else fails, get out the correlation chart, the average accuracy is 99.39%, average sensitivity is 99.92%, average DER is 0.0067% and positive predictivity is 99.39% of the different data bases are calculated.

Keywords: ECG, PPG, PRV, AVNN, SDNN, SDDSD, RMSSD, pNN20, pNN50, VLF, LF, HF, LF/HF.

1. INTRODUCTION

Heart and blood vessel issues are a part of cardiovascular illnesses (CVDs). The majority of sudden cardiac deaths are due to these illnesses. The best way to prevent cardiovascular illnesses is through early detection of aberrant cardiac events. Automated, trustworthy clinical feature extraction technology has recent. The most crucial function in increasing the computer-aided cardiovascular diagnostic system's diagnostic accuracy is played

by prediction approaches. The promise of continuous monitoring and early cardiovascular event prediction is furthered by current sensor innovation breakthroughs in wearable medical devices. Thus, methods for reliable detection of cardiac events in wearable devices should minimise power consumption[1-5]. Predicting abrupt cardiac events is also possible. As a consequence of the sympathetic and parasympathetic nervous systems, clinical metrics derived from ECG and PPG signals may give valuable insight into the operation of the cardiac system. Variation in the duration between systolic peaks in a photoplethysmography (PPG) signal constitutes pulse rate variability (PRV), a physiological phenomenon[5-7]. It's a way to quantify how much a signal's pulse interval varies from one iteration to the next. In particular, its variability provides very significant physiological information for cardiac diagnosis. Photoplethysmography (PPG) is an optical noninvasive method for measuring relative arterial blood volume changes from one heartbeat to the next. PPG signals are pulsating waveforms that show variations in blood volume and vascular abnormalities in the fingers. Time-frequency indices derived from the PPG signal are very sensitive to even subtle changes in

autonomic nervous system function because of the rapid feedback loop between the two. Amplitude, baseline, time period, dicrotic peak, and dicrotic notch are all aspects of the PPG waveform that are essential for evaluating autonomic nervous system function and diagnosing heart disorders[10-15].

1.1 PPG:

An optically obtained plethysmogram, also known as a "photo plethysmogram," can be used to gauge changes in the blood volume in the microvascular bed. PPG is an easy and affordable optical technique for tracking changes in the blood volume in the microvascular bed. Electrocardiogram with pulsatile component and photoplethysmograph (PPG) signal. It is frequently employed for non-invasive measuring near the skin's surface[15-17]. The PPG's pulsating physiological waveform, also known as an "AC" waveform, is brought on by changes in blood volume brought on by heartbeats. Lower frequency components of this waveform, which are superimposed over a slowly fluctuating (referred to as a "DC") baseline, are linked to breathing, sympathetic nervous system activity, and thermoregulation. Although it is well acknowledged that the PPG signal may shed light on the cardiovascular system, it is still unknown where its constituent parts came from.

By measuring the distance between character sequences using both local and global data, it is possible to distinguish anomalies in PPG signals. It is considered an aberrant pattern when the separation exceeds a specific value. A wide range of physiological data may be analyzed using the suggested method[17-19].

1.2 PRV:

Blood volume pulse (BVP) signals are measured using photoplethysmography, and "pulse rate variability" (PRV) is the term used to describe variations in the duration between each BVP (PPG). The state of a person's autonomic nervous system may be gauged by measuring their pulse wave velocity (PRV). For an accurate method of gauging BVP, please contact PPG (CPPG). CPPG may be uncomfortable for the user since the sensor used for measurements is attached to their finger. Pulse rate (PR) variability (PRV) is the result of ANS alterations in response to changes in the internal and external environment[5,8,10,15]. PRV reflects transient PR and PPI fluctuations and is linked to the interactions between the sympathetic and parasympathetic nerves affecting the sinus node[20-25]. For PRV analysis, the PR signal is commonly recorded through electrocardiography (ECG) or a continuous invasive pulmonary artery

pressure (CPPG) sensor. The PRV parameters like AVNN, SDNN, SDSD, RMSSD, pNN20, pNN50, VLF, LF, HF, LF/HF ratio are calculated.

2. PROPOSED ALGORITHM

In this section we are using the algorithm to detect the R peak. This includes the steps

- Bandpass Filtering and Differentiation
- New Nonlinear Transformation
- New Peak-Finding Technique
- Finding Location of True R-Peaks

Bandpass Filtering and Differentiation

ECG signals are commonly obscured in real-world settings by a variety of environmental sounds and artefacts. Power line interference, muscle contractions, baseline drift from breathing, and fast baseline shift are only few of the major ECG noise sources that may severely taint ECG data. The bulk of a QRS complex's frequency information is between 5 and 30 hertz. Up to 5 Hz, P/T waves and motion artefacts concentrate the vast majority of their noise energy. Hence, adequate P/T wave and noise suppression up to 5 Hz is necessary. The bulk of the frequencies in the QRS complex are under 20 Hz, as shown by a spectral analysis of the various QRS geometries with durations between 0.05 and 0.2 s. The passband was used in this study to optimise the energy of various QRS complexes while reducing the influence of P/T waves, powerline interference, motion artefacts, and muscle noise (narrow-QRS and wide-QRS complexes).

Using the least-squares method, we build a 15th-order FIR bandpass DF with cutoff frequencies of 6 and 20 Hz for the passband. When we apply a filter to the filtered QRS complex, we use first-order forward differentiation to bring out the steep slopes and high frequencies. The following are the distinguishing features of $f[n]$:

$$d[n] = f[n+1] - f[n]$$

New Nonlinear Transformation

Squaring and Adaptive Thresholding

Afterwards, adaptive thresholding is applied to the energy (or squarer) values of $e[n]$. After squaring the dECG signal $d[n]$, a positive-valued signal is obtained. The squaring is performed by applying an adaptive

threshold to the energy (or squarer) values of $e[n]$. To produce a positive-valued signal, the dECG signal $d[n]$ is first squared. The squaring off is done by

$$e[n] = d^2[n]$$

The thresholding function is defined as

$$e_{th}[n] = \begin{cases} 0, & e[n] < g \\ e[n], & otherwise \end{cases}$$

If an energy value, $e[n]$, is less than the threshold parameter g , it is reduced to zero and the remaining values are kept. Here, we determine the g value for each ECG segment as its adaptive threshold parameter.

$$n = 0.5 * \sigma_e$$

$$\text{where } \sigma_e = \sqrt{\frac{1}{M} \sum_{m=1}^M (e[n] - \alpha)^2} \text{ and } \alpha = \frac{1}{M} \sum_{m=1}^M e[n]$$

Shannon Energy Computation and Smoothing

The Shannon energy values are smoothed using a finite-impulse response (FIR) filter with a rectangular impulse response $h[k]$ of length L in order to lessen the prominence of multiple peaks in the QRS complex. The target peaks of this smoothing process are the subdivisions of the QRS-complex. A smooth feature signal is the end result of the suggested nonlinear transformation. It is possible to see that the putative R-peaks in the SE envelope $s[n]$ are roughly located where they are in the provided ECG waveform. To find the actual R peaks in an ECG signal, it is suggested to analyse these candidate R peaks. There are slight changes between succeeding R peaks as a result of the Shannon energy transition. We investigated the performance of this nonlinear transformation in previous work. Findings from experiments show that it may enhance the accuracy of detecting ECG signals with both small and big QRS complexes. Then, the signal's threshold energy must be normalised as

$$\overline{e_{th}}[n] = \frac{e_{th}[n]}{\max_{m=1}^M (e_{th}[n])}$$

And Shannon energy of the normalized signal $\overline{e_{th}}[n]$ is computed as

$$s[n] = -\overline{e_{th}}^2[n] \log_e \overline{e_{th}}^2[n]$$

An FIR filter with a rectangular impulse response $h[k]$ of length L is used to smooth out the Shannon energy values, reducing the influence of numerous peaks in the vicinity of the QRS complex. The desired result of this smoothing technique is a series of peaks that map to the QRS-complex sub-components. It is proposed that a nonlinear transformation be used to produce a signal with symmetrical features. Rough R peak

positions in the ECG waveform are also roughly correlated with the anticipated R-peak sites in the SE envelope $s[n]$. When applied to an ECG signal, our proposed technique identifies the true R peaks by performing further processing on the candidate peaks.

New Peak-Finding Technique

The first-order Gaussian differentiator (**FOGD**) operator is used in this section's unique and simple peak-finding method to automatically locate probable R-peaks in the SE envelope. The First-Order Gaussian Differentiator

Here N point Gaussian window $w[n]$ is defined as

$$w[n] = e^{-\frac{1}{2} \left(\frac{n - \frac{N}{2}}{\rho} \right)^2} \text{ where, } n = 1, 2, 3, \dots, N$$

And FOGD is written as

$$w_d[n] = w[n+1] - w[n], \text{ where } n = 1, 2, 3, \dots, N-1$$

The slope at each sample is depicted as the 901-point Gaussian window with spread $r = 36$, and the associated FOGD function.

The first order derivative of the Gaussian window is an asymmetric function and is symmetric at $[N/2] + 1$. Moreover, the peak of the Gaussian window function occurs at $n = [N/2] + 1$. As a result, the slope of FOGD is zero for $n = N/2$ and has positive and negative values for $1 \leq n \leq N/2$ and $N/2 + 1 \leq n \leq N$. On this, the suggested peak-finding logic is predicated. To find probable R-peaks in the SE envelope, we convolution the FOGD sequence $w_d[m]$ with the SE envelope $s[n]$. Furthermore, FOGD sequence is calculated as

$$Z[n] = \sum_{l=-\infty}^{\infty} w_d[l] s[n-l]$$

For the result of a convolution between the **FOGD** function's output and a Shannon energy envelope. Due to the asymmetric nature of the **FOGD** function, the resulting convolution is referred to as the **ZC** function $z[n]$ in this study, where n is an integer. When the signal goes from negative to positive, it causes a positive **ZC** (zero crossing) with a positive slope. When the signal $z[n]$ flips from positive to negative, the resulting **ZC** has a negative slope and is negative in magnitude. Peaks in the Shannon energy envelope $s[n]$ may be shown to be located at negative **ZCs**, as shown in Figure 5c. This leads to the discovery and use of negative **ZCs**.

Detecting Negative Zero-crossings

Analysis of the sign of the **ZC** function at time instants t_n and t_{n+1} reveals the existence of negative **ZCs** in this investigation. The proposed peak-finding approach

correctly positions the possible R-peaks in the SE envelope in time. As compared to the observed time instants, the true R peaks in the ECG signal are somewhat off. When candidate R-peaks have been found, their timestamps are utilised as references to find the real R-peaks in the subsequent phase.

Locating the Real R-Peaks

This step use the positions of each potential R-peak found in the previous step to pinpoint the precise times at which R-peaks appear in the original ECG signal. Reconstructing the original ECG signal begins with locating the origin of each potential R-peak. The section's largest peak value is then identified by a straightforward process. These steps are repeated m times for each of the possible places p. The findings demonstrate that accurate R-peak locations may be obtained even when noise and irregular QRS complexes are present.

Algorithm Implementation and Assessment

The aforementioned technique is run in MATLAB at 2.4 GHz on an Intel Core 2 Quad processor. The technique is tested on data from the MIT-BIH arrhythmia database and the slpdb [26] signals database (<https://archive.physionet.org/physiobank/database/>). Combining the two subsequent R-peaks in the ECG signal requires a bigger value of M. The length of the smoothing filter was found to be an average of the minimum and maximum QRS complex durations. Normal and broad QRS complexes last between 0.05 and 0.2 seconds. To determine the length of the smoothing filter, a sampling rate of 360 samples per second is used. Sensitivity, accuracy, predictability, and the percentage of false positives in detection are all under scrutiny. The Se measures how well the algorithm can identify actual R-peaks out of all R-peaks in the original ECG signal. The +P is the fraction of true R-peaks among all algorithm-assigned peaks.

$$Se = TP / (TP + FN) * 100 \%$$

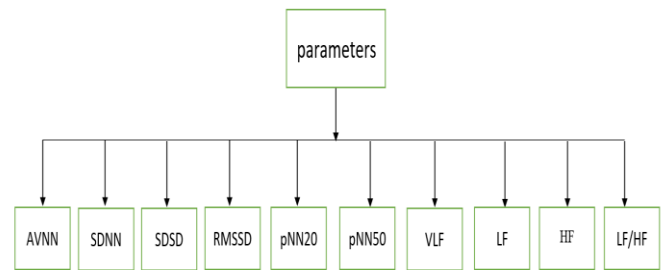
$$Acc = TP / (TP + FP + FN) * 100\%$$

$$P = TP / (TP + FP) * 100\%$$

$$DER = (FP + FN) / TP * 100\%$$

Parametry Detection

There are some parameters which are required to detect after peak detection. They are:



PARAMETERS	ABBREVIATIONS
AVNN	Average of NN Intervals
SDNN	Standard Deviations of NN Intervals
SDD	Standard Deviations of Successive Differences
RMSSD	Root Mean Square of Successive Differences between normal heartbeats
pNN20	Proportion of NN20 divided by total no. of NNs
pNN50	Proportion of NN50 divided by total no. of NNs
VLF	Very Low Frequency
LF	Low Frequency
HF	High Frequency
LF/HF	Ratio of Low Frequency to High Frequency

Fig 2.1:PRV parameters

AVNN: It is a measurement of the typical beat interval between systolic beats that is calculated in milliseconds (ms). This parameter is measured as

$$AVNN = \bar{m} = \frac{1}{N-1} \sum_{n=2}^N D(n)$$

SDNN: Standard deviation for all NN intervals, calculated in milliseconds, is measured by SDNN (ms). It can alternatively be described as the square root of variance computed on the times between peaks. Because of this, the parameter that is mathematically comparable to the total power estimated on the PPG signal spectrum. Longer records are necessary for a more accurate SDNN value because the accuracy of the SDNN depends on the length of the data. This parameter is most helpful for patients with AMI and CHF, and determining the relative importance of the sympathetic and parasympathetic neural systems in regulating blood flow using this information.

$$SDNN = \sqrt{\frac{1}{N-1} \sum_{n=2}^N [D(n) - \bar{m}]^2}$$

SDSD: It's the milliseconds(ms).-based standard deviation of two successive NN intervals.

RMSSD: It is a measurement of the root mean square difference between two consecutive peak intervals. The parasympathetic control of the heart is assessed using high frequency fluctuations in this measure. It is measured as

$$RMSSD = \sqrt{\frac{1}{N-2} \sum_{n=3}^N [D(n) - D(n-1)]^2}$$

pNN20: It is a measure of how often neighboring NN intervals in the full PPG recording have a difference of more than 20 ms. The primary function of this parameter is to measure the parasympathetic behaviour governed by the autonomic nerve system. You may calculate it by

$$pNN20 = \frac{\text{total NN20 count}}{\text{total NNcount}}$$

pNN50: It is a measure of how often neighbouring NN intervals in the full PPG recording have a difference of more than 50 ms. The primary function of this parameter is to measure the parasympathetic activity of the autonomic nervous system. It is measured as

$$pNN50 = \frac{\text{total NN50 count}}{\text{total NNcount}}$$

LF Norm: The normalized value for LF band power computed as

$$LF \text{ Norm} = \frac{LF}{\text{Total power-VLF}} \times 100$$

HF Norm: The normalized value for HF band power computed as

$$HF \text{ Norm} = \frac{HF}{\text{Total power-VLF}} \times 100$$

3. METHODOLOGY:

PPG Measurement: For the aim of monitoring heart rate, photoplethysmography (PPG) is a common and low-cost optical measuring method. Blood volume changes may be detected using a device called photoplethysmography (PPG), which uses a light source and a photodetector on the skin's surface.

Heartbeat Detection:Electrocardiogram (ECG) is routinely used to assess heartbeats. Arrhythmia is a disruption of the heartbeat that may possibly be deadly. Arrhythmia may be identified by recognising an

individual aberrant heartbeat, which can occur in isolation or consecutively.

Heartbeat Qualification:Your heart rate is the number of times per minute that your heart beats, which is generally between 60 and 100 times per minute for people.

NN-Interval statistics: Each QRS complex in a continuous ECG recording is identified, and the so-called normal-to-normal (NN) intervals—all gaps in between successive QRS complexes resulting from sinus node depolarizations—or the instantaneous heart rate are then calculated.

- Method of calculation: The time difference between the QRS and the preceding QRS.
- The NN interval is based on the RR interval where untrustworthy RR intervals are removed. Moreover, an RR interval varying by more than 150ms from the 5 neighboring intervals is also eliminated.
- Frequency: Async
- Source data: ECG
- Quality: NN intervalstatusCVS
- Unit: seconds

Interpretation of Status: Your heart's variability reveals how adaptive your body can be. If your heart rate is very varied, this is typically indicative that your body can adjust to numerous sorts of changes. People with high heart rate variability are frequently less anxious and happy.



Fig1: Block diagram

SYSTOLIC PEAKS CALCULATION TABLE:

Record	TP	FP	FN	Sensitivity	Accuracy	DER	positive predictivity
a01erm	10,958	79	2	99.98	99.26	0.0073	99.28
a01m	10,904	71	2	99.98	99.33	0.0066	99.35
a02erm	13,482	9	19	99.85	99.79	0.002	99.85
a02m	13,445	27	24	99.82	99.62	0.003	99.79
a03m	10,844	94	0	100	99.14	0.0086	99.14
a04erm	11,435	58	8	99.93	99.42	0.005	99.49
a04m	11,433	60	5	99.95	99.43	0.005	99.47
a05m	11,029	73	2	99.98	99.32	0.006	99.34
a06m	10,741	90	4	99.96	99.13	0.008	99.16
a07m	12,327	52	0	100	99.57	0.004	99.57
a08m	13,973	29	0	100	99.79	0.002	99.18
a09m	10,399	86	0	100	99.17	0.008	99.17
a10m	10,649	64	2	99.98	99.38	0.006	99.4
a11m	12,142	73	14	99.88	99.28	0.007	99.4
a12m	11,242	68	1	99.99	99.38	0.006	99.39
a13m	10,342	79	3	99.97	99.21	0.007	99.24
a14m	12,465	92	0	100	99.26	0.007	100

a15m	11,496	78	12	99.89	99.22	0.007	99.32
a16m	10,790	68	8	99.92	99.3	0.007	99.37
a17m	13,499	27	15	99.98	99.68	0.003	99.8
a18m	12,273	58	5	99.95	99.48	0.005	99.52
a19m	10,908	45	16	99.85	99.44	0.005	99.58
a20m	10,849	86	12	99.88	99.1	0.009	99.21
b01erm	11,941	63	20	99.83	99.3	0.006	99.47
b01m	11,939	65	12	99.89	99.35	0.006	99.45
b02m	11,596	74	18	99.84	99.21	0.007	99.36
b03m	11,996	72	14	99.88	99.28	0.007	99.4
b04m	10,998	79	16	99.85	99.14	0.008	99.28
b05m	10,956	84	18	99.83	99.07	0.009	99.23
c03m	8837	79	1	99.98	99.1	0.009	99.11
c01erm	7750	32	0	100	99.58	0.004	99.58
c01m	7249	74	2	99.97	99.96	0.01	99.98
c02erm	7439	46	0	100	99.38	0.006	99.38
c02m	8439	64	2	99.97	99.22	0.007	99.24
c03erm	7229	38	12	99.83	99.31	0.006	99.47
c04m	8539	78	19	99.77	99.87	0.011	99.09
c05m	8445	76	5	99.94	99.04	0.009	99.1
c06m	8794	92	14	99.84	99.8	0.012	99.96
c07m	7996	43	0	100	99.46	0.005	99.46
c08m	8884	82	4	99.95	99.04	0.009	99.08
c09m	7924	79	11	99.86	99.87	0.011	99.01
c10m	8939	82	17	99.81	99.9		99.09

Fig 3.1 Detection of Systolic peaks for different databases

TSP= Total systolic peaks
 FP=False positive
 FN=False negative
 Se= Sensitivity
 Acc= Accuracy
 P= Predictivity
 DER= Detection error rate

4. RESULTS

4.1 PRV Result Analysis:

The proposed work is tested and analyzed with different databases and real time signals. The various parameters are calculated using formulas. The parameters include systolic peak amplitude, systolic peak time, peak to peak interval, AVNN, SDNN, RMSDD, SDSD, pNN20, pNN50, VLF, LF, HF and LF/HF ratio.

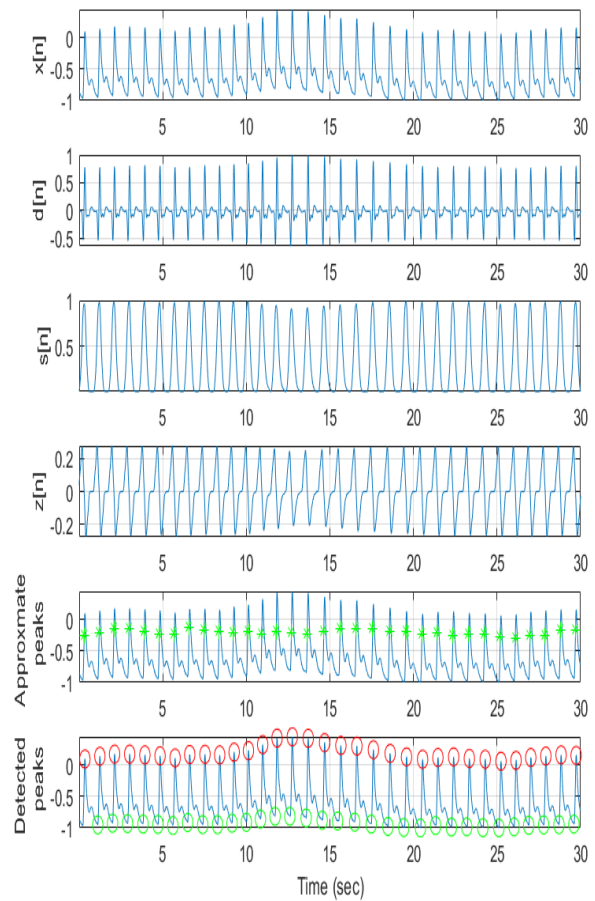


Fig4.1.1: Peak detection of the PPG signal using proposed algorithm for the systolic peaks in 30 secs of time. Here $x[n]$ is original signal, $d[n]$ is difference of filtered signal, $s[n]$ is Shannon Energy, $z[n]$ is Gaussian Energy.

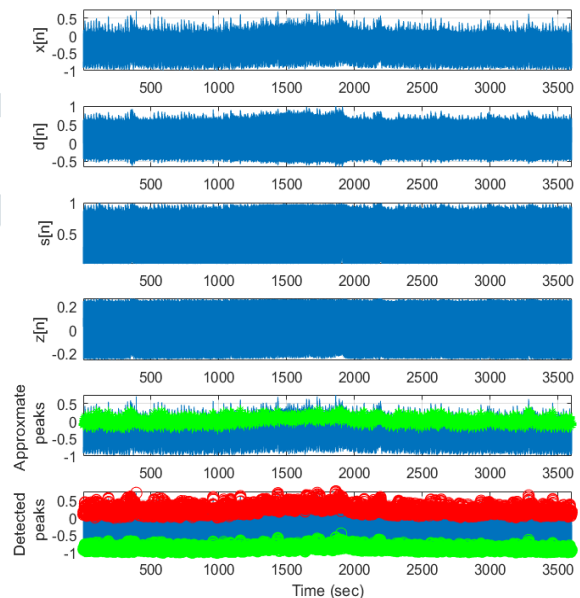


Fig4.1.2: Peak detection of the PPG signal using proposed algorithm for the systolic and d peaks in 3600 secs of time.

Fig: 4.2.1PRV parameter values

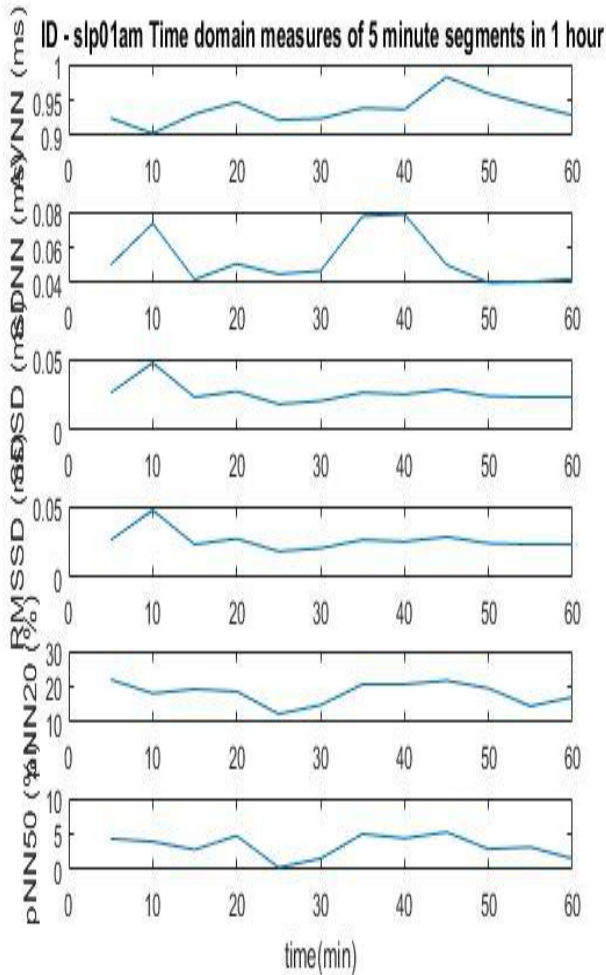


Fig: 4.1.3PRV parameters in time domain

5. CONCLUSION

In this study, we proposed a unique systolic peak and onset identification method for the automatic PPG data processing. This work presents a simple method for automated R-peak detection in an electrocardiogram. This method uses novel transformations along with simple peak-finding techniques. The accuracy of our findings is quite high; we have successfully reduced both false positives and false negatives by a significant margin. Peak detection on the positive signals is done after the noise signals are attenuated. The proposed system analyses a wide range of signals, including both real-time and database-stored signals. The various signals are analysed for a total of 60 minutes. The signal determines the accuracy rate, which varies. Our research, however, demonstrates that 99% accuracy is frequently attained by all signals. Finally, for the correlation analysis, the average accuracy is 99.39%, average sensitivity is 99.92%, average DER is 0.0067% and positive predictivity is 99.39% of the different data bases are calculated.

REFERENCES

- [1] Bansal, Dipali, Munna Khan, and A. K. Salhan. "A review of measurement and analysis of heart rate variability." In *2009 International Conference on Computer and Automation Engineering*, pp. 243-246. IEEE, 2009.
- [2] Lin, Wan-Hua, Dan Wu, Chunyue Li, Heye Zhang, and Yuan-Ting Zhang. "Comparison of heart rate variability from PPG with that from ECG." In *The International Conference on Health Informatics: ICHI 2013, Vilamoura, Portugal on 7-9 November, 2013*, pp. 213-215. Springer International Publishing, 2014.
- [3] Lu, Sheng, He Zhao, Kihwan Ju, Kunson Shin, MyoungHo Lee, Kirk Shelley, and Ki H. Chon. "Can photoplethysmography variability serve as an alternative approach to obtain heart rate variability information?" *Journal of clinical monitoring and computing* 22 (2008): 23-29.
- [4] Lulkar, Rutuja, and Nivedita Daimiwai. "Acquisition of PPG signal for diagnosis of parameters related to heart." In *2012 1st International Symposium on Physics and Technology of Sensors (ISPTS-1)*, pp. 274-277. IEEE, 2012.
- [5] Logier, Régis, A. Dassonneville, and M. Jeanne. "Comparison of pulse rate variability and heart rate variability for high frequency content estimation." In *2016 38th Annual International Conference of the IEEE Engineering in Medicine and Biology Society (EMBC)*, pp. 936-939. IEEE, 2016.

4.2PRVParameters Result Analysis:

The proposed work is tested and analyzed with different databases and real time signals. The various parameters are calculated using formulas. The parameters include systolic peak amplitude, systolic peak time, peak to peak interval, AVNN, SDNN, RMSDD, SDSD, pNN20, pNN50, VLF, LF, HF and LF/HF ratio. Here AVNN(ms) value is 936.66 +/- 19.37.

PARAMETERS	VALUES
AVNN (ms)	936.66 +/- 19.37
SDNN (ms)	53.10 +/- 13.98
SDSD (ms)	26.13 +/- 6.93
RMSDD (ms)	26.13 +/- 6.93
pNN20 (%)	18.29 +/- 2.92
pNN50 (%)	3.32 +/- 1.50
VLF (msec ²)	1160.35 +/- 1136.67
LF (msec ²)	1233.10 +/- 329.41
HF (msec ²)	217.57 +/- 95.46
LF (n.u.)	0.84 +/- 0.05
HF (n.u.)	0.15 +/- 0.05
LF/HF (ratio)	6.88 +/- 3.56

- [6] Moody, George B., and Roger G. Mark. "The impact of the MIT-BIH arrhythmia database." *IEEE engineering in medicine and biology magazine* 20, no. 3 (2001): 45-50.
- [7] Khattak, Hasan Ali, Michele Ruta, and Eugenio Eugenio Di Sciascio. "CoAP-based healthcare sensor networks: A survey." In *Proceedings of 2014 11th International Bhurban Conference on Applied Sciences & Technology (IBCAST) Islamabad, Pakistan, 14th-18th January, 2014*, pp. 499-503. IEEE, 2014.
- [8] Padikkapparambil, Jinesh, Cornelius Ncube, Krishna Kant Singh, and Akansha Singh. "Internet of Things technologies for elderly health-care applications." In *Emergence of pharmaceutical industry growth with industrial IoT approach*, pp. 217-243. Academic Press, 2020.
- [9] Tadoju, Shirisha, and J. Mahesh. "Bluetooth remote home automation system using Android application." *International Journal of Advanced Technology and Innovative Research*, ISSN 23 (2015): 48-2370.
- [10] Mohanty, Abhinav, Islam Obaidat, Fadi Yilmaz, and Meera Sridhar. "Control-hijacking vulnerabilities in IoT firmware: A brief survey." In *The 1st International Workshop on Security and Privacy for the Internet-of-Things (IoTSec)*. 2018.
- [11] Negra, Rim, Imen Jemili, and Abdelfettah Belghith. "Wireless body area networks: Applications and technologies." *Procedia Computer Science* 83 (2016): 1274-1281.
- [12] Mathew, Avin, Sheng Zhang, Lin Ma, Tom Earle, and Douglas Hargreaves. "Reducing maintenance cost through effective prediction analysis and process integration." *Advances in vibration engineering* 5, no. 2 (2006): 87-96.
- [13] Corrado, Domenico, Cristina Basso, Maurizio Schiavon, Antonio Pelliccia, and Gaetano Thiene. "Pre-participation screening of young competitive athletes for prevention of sudden cardiac death." *Journal of the American college of cardiology* 52, no. 24 (2008): 1981-1989.
- [14] Shahkar, Shahram, Yanyan Shen, and Khashayar Khorasani. "Diagnosis, prognosis and health monitoring of electro hydraulic servo valves (EHSV) using particle filters." In *2019 6th International Conference on Control, Decision and Information Technologies (CoDIT)*, pp. 385-390. IEEE, 2019.
- [15] Blum, Jeremy. *Exploring Arduino: tools and techniques for engineering wizardry*. John Wiley & Sons, 2019.
- [16] Tang, Xilang, Xueqi Wang, Mingqing Xiao, Kai Leung Yung, and Bin Hu. "Health condition estimation of spacecraft key components using belief rule base." *Enterprise Information Systems* 15, no. 8 (2021): 1107-1127.
- [17] Anand, Sakshi, and Avinash Sharma. "Assessment of security threats on IoT based applications." *Materialstoday: proceedings* (2020).
- [18] Yu, Enze, Dianning He, Yingfei Su, Li Zheng, Zhong Yin, and Lisheng Xu. "Feasibility analysis for pulse rate variability to replace heart rate variability of the healthy subjects." In *2013 IEEE International Conference on Robotics and Biomimetics (ROBIO)*, pp. 1065-1070. IEEE, 2013.
- [19] Ghamari, Mohammad, Christopher Aguilar, C. Soltanpur, and Homer Nazeran. "Rapid prototyping of a smart device-based wireless reflectance photoplethysmograph." In *2016 32nd Southern Biomedical Engineering Conference (SBEC)*, pp. 175-176. IEEE, 2016.
- [20] Mohan, P. Madhan, V. Nagarajan, and Sounak Ranjan Das. "Stress measurement from wearable photoplethysmographic sensor using heart rate variability data." In *2016 International Conference on Communication and Signal Processing (ICCSP)*, pp. 1141-1144. IEEE, 2016.
- [21] Chou, Yongxin, Peiyi Zhu, Xufeng Huang, Jiajun Lin, Jicheng Liu, and Ya Gu. "Comparison between heart rate variability and pulse rate variability for bradycardia and tachycardia subjects." In *2018 International Conference on Control, Automation and Information Sciences (ICCAIS)*, pp. 1-6. IEEE, 2018.
- [22] Joshi, Aniruddha J., Sharat Chandran, Valadi K. Jayaraman, and Bhaskar D. Kulkarni. "Arterial pulse rate variability analysis for diagnoses." In *2008 19th International Conference on Pattern Recognition*, pp. 1-4. IEEE, 2008.
- [23] Malik, Anshul, and R. K. Sharma. "Detection of heart conditions using HRV processor in Matlab simulink." In *2017 International Conference on Trends in Electronics and Informatics (ICEI)*, pp. 861-864. IEEE, 2017.
- [24] Béres, Szabolcs, Lőrinc Holczer, and László Hejmel. "On the minimal adequate sampling frequency of the photoplethysmogram for pulse rate monitoring and heart rate variability analysis in mobile and wearable technology." *Measurement Science Review* 19, no. 5 (2019), pp.232-240.
- [25] McKinley, Paula S., Peter A. Shapiro, Emilia Bagiella, Michael M. Myers, Ronald E. De Meersman, Igor Grant, and Richard P. Sloan. "Deriving heart period variability from blood pressure waveforms." *Journal of Applied Physiology* 95, no. 4 (2003): 1431-1438.
- [26] <https://archive.physionet.org/cgi-bin/atm/ATM>.